JVI Journals.ASM.org

Genomic Characterization of Japanese Macaque Rhadinovirus, a Novel Herpesvirus Isolated from a Nonhuman Primate with a Spontaneous Inflammatory Demyelinating Disease

Ryan D. Estep,[a] Scott G. Hansen,[a] Kelsey S. Rogers,[a] Michael K. Axthelm,[a,b] Scott W. Wong[a,b,c]

Vaccine and Gene Therapy Institute, Oregon Health and Science University, Beaverton, Oregon, USA[a]; Division of Pathobiology and Immunology, Oregon National Primate Research Center, Beaverton, Oregon, USA[b]; and Department of Molecular Microbiology and Immunology, Oregon Health and Science University, Portland, Oregon, USA[c]

Japanese macaque rhadinovirus (JMRV) is a novel gamma-2 herpesvirus that was isolated from a Japanese macaque (JM) with an inflammatory demyelinating encephalomyelitis referred to as Japanese macaque encephalomyelitis, a disease that possesses clinical and histopathological features resembling multiple sclerosis in humans. Genomic DNA sequence analysis reveals that JMRV is a gammaherpesvirus closely related to rhesus macaque rhadinovirus (RRV) and human herpesvirus 8. We describe here the complete nucleotide sequence and structure of the JMRV genome, as well as the sequence of two plaque isolates of this virus. Analysis of the JMRV genome not only demonstrates that this virus shares a number of genes with RRV that may be involved in pathogenesis but also indicates the presence of unique JMRV genes that could potentially contribute to disease development. The knowledge of the genomic sequence of JMRV, and the ability to easily propagate the virus *in vitro*, make JMRV infection of JM an attractive model for examining the potential role of an infectious viral agent in the development of demyelinating encephalomyelitis disease *in vivo*.

We recently described the occurrence of a spontaneous demyelinating disease that possesses clinical and histopathological features resembling multiple sclerosis (MS) in a colony of Japanese macaques (JM; *Macaca fuscata*) housed at the Oregon National Primate Research Center (1). This disease, referred to as Japanese macaque encephalomyelitis (JME), presents with clinical features such as ataxia and paralysis and, in some cases, is associated with episodes of recovery and relapse. Magnetic resonance imaging of several JME cases revealed multiple gadolinium-enhancing T_1-weighted hyperintensities in the white matter of the cerebral hemispheres, cerebella, brainstems, and cervical spinal cords of animals. Histopathological similarities with MS were also observed and were characterized by the presence of multifocal plaque-like demyelinated lesions accompanied with inflammatory cell infiltrates and loss of oligodendrocytes and axons. Of particular interest was the isolation of a novel gammaherpesvirus, referred to as Japanese macaque rhadinovirus (JMRV), from a central nervous system (CNS) lesion of a JM that had developed JME (1). JMRV was subsequently found in other JME lesions but not in normal white matter tissue of affected animals, suggesting the virus is a passenger within the inflammatory cells infiltrating the lesion or may be associated with the development of JME. We report here the complete sequence and structure of the JMRV genome, as well as two plaque isolates of this virus, and demonstrate that JMRV is closely related to other primate gammaherpesviruses, while also possessing unique features. The expression pattern of several JMRV-unique open reading frames (ORFs) is also examined.

MATERIALS AND METHODS

Viral genomic DNA isolation. The identification and preliminary characterization of JMRV strain 17792 ($JMRV_{17792}$) was previously described (1). $JMRV_{17792}$ is referred to throughout the present study as JMRV. To isolate purified viral genomic DNA for sequence analysis, primary rhesus fibroblasts were seeded in 850-cm^2 roller bottles, infected at a multiplicity of infection (MOI) of 0.01, and incubated until the appearance of full cytopathic effect. Next, the cells and supernatants were collected and subjected to centrifugation at 1,000 × *g* for 10 min. The clarified supernatants were then collected, the cell pellet was sonicated and spun at 1,000 × *g* for 10 min, and all clarified supernatants were pooled. The virus was then pelleted from supernatants by centrifugation at 12,500 × *g* for 1 h at 4°C, and the resulting pellet was resuspended in 1 ml of 1 mM Tris-HCl (pH 8.0)-1 mM EDTA (TE) and added to the top of a six-step sorbitol gradient, ranging from 20 to 70%. The gradients were spun in a Beckman SW41 rotor for 2 h at 18,000 rpm at 4°C. The virus-containing band at the 50 to 60% interface was collected and diluted with 15 ml of cold 1 mM Tris-HCl and then pelleted by centrifugation in the SW41 rotor for 50 min at 18,000 rpm at 4°C. The washed virus pellet was resuspended in 9.2 ml of TE (pH 8.0), and particles were digested at 37°C overnight in 0.6 ml of 10% sodium dodecyl sulfate and 0.2 ml of proteinase K (10 mg/ml) to release the viral DNA. Finally, the viral DNA was purified by $CsCl_2$ gradient centrifugation in a Beckman Ti75 rotor at 38,400 rpm for 72 h, and the collected fractions were dialyzed against TE (pH 8.0).

Sequence analysis of the JMRV genome. To facilitate DNA sequencing of the JMRV genome, a shotgun subclone library was generated, and the DNA sequence of the viral genome was determined essentially as described previously for rhesus cytomegalovirus (2). Using this approach, the entire genome was sequenced with a 6-fold redundancy. The complete sequence for JMRV is available in GenBank under accession number AY528864.

Analysis of JMRV ORFs. ORFs were identified with MacVector software (MacVector, Inc., Cary, NC), and the target search criterion for an

Received 16 August 2012 **Accepted** 16 October 2012
Published ahead of print 24 October 2012
Address correspondence to Scott W. Wong, wongs@ohsu.edu.

doi:10.1128/JVI.02194-12

ORF was DNA sequence encoding a protein of at least 80 amino acids (aa). The ORFs that were identified in this manner were translated and analyzed using the BLASTP tool from the NCBI using default parameters to identify other known proteins with homology.

Sequence alignments and phylogenetic analysis. Sequence alignments were performed with CLUSTAL W, and phylogenetic analysis was performed by bootstrap analysis with the neighbor-joining method, using MacVector software. Herpesvirus DNA polymerase protein sequences utilized in phylogenetic analysis were obtained from GenBank (herpesvirus saimiri [HVS], CAA45632; human herpesvirus 8 [HHV-8], AAC57086; Epstein-Barr virus [EBV] YP_401712; rhesus lymphocryptovirus, YP068007; murine herpesvirus 68 [MHV-68], AAB66388; rhesus macaque rhadinovirus [RRV], AAD21336; JMRV, AAS99991).

Terminal repeat (TR) identification. Restriction digest analysis was performed by digesting 2 μg of viral DNA with enzyme overnight at 37°C and analyzing the products on a 1% agarose gel containing ethidium bromide. An ~1.6-kb HindIII restriction fragment was identified and excised from the gel, purified using a Zymoclean gel DNA recovery kit (Zymo Research, Irvine, CA), and cloned into vector pSP73 (Promega, Madison, WI) digested with the same enzyme. A clone containing the insert was identified, and plasmid DNA was then isolated and sequenced.

Analysis of unique JMRV ORF expression. Primary rhesus fibroblasts were infected with JMRV at an MOI of 5, and individual cultures were then treated with 75 μg of cycloheximide (CHX)/ml to inhibit protein synthesis, 7.5 μM ganciclovir (GCV) to inhibit DNA replication, or left untreated to allow the definition of gene expression as immediate-early, early, or late, respectively. The time points for collection of RNA were 24 h (+CHX), 48 h (+GCV), and 72 h (untreated), since these three classes of genes are expressed at these approximate time points after JMRV infection *in vitro*. RNA from mock-infected cells collected at 72 h served as a negative control for all reactions. RNA was isolated from infected cells using TRI Reagent (Sigma-Aldrich, St. Louis, MO). Reverse transcription-PCR (RT-PCR) was performed with a Superscript III One-Step RT-PCR System (Life Technologies, Grand Island, NY) and gene-specific primers designed to amplify the precise length of each predicted ORF, and the resulting reactions were run on a 1.7% agarose gel. Analysis of secretion signals for each predicted protein were performed with the SignalP 4.0 server (3) and the Secretome 2.0 Server (4; http://www.cbs.dtu.dk/services).

Sequence analysis of JMRV plaque isolates. Plaque-purified isolates of JMRV were obtained by dilution of the original stock of virus on primary rhesus fibroblasts and picking single plaques. After two further rounds of plaque purification, two isolates (denoted 3A1 and 12E2) were identified and selected for propagation and analysis. Stocks of each virus were grown in primary rhesus fibroblasts, and viral DNA was isolated using procedures described above. Next, short read sequence analysis of the purified viral DNA was performed by the OHSU Massively Parallel Sequencing Shared Resource using an Illumina GA IIx sequencer, and the resulting reads were computationally assembled into a consensus sequence for each viral genome using the program Velvet. Using this method, an estimated 300-fold depth of coverage was achieved for each nucleotide in the viral genome. Any apparent gaps in genomic sequences introduced as a result of errors in the assembly process were confirmed by PCR, using purified viral DNA as a template and unique primers flanking each region. PCR products resulting from these analyses were purified and directly sequenced, and the genomic sequences were then manually edited to reflect the correct sequence at these locations.

RESULTS

Sequence analysis of the JMRV genome. To determine the complete sequence of JMRV, a shotgun subclone library spanning the entire genome was generated from purified viral genomic DNA using methods described previously (5). Next, individual clones were sequenced, and the resulting reads were assembled into a consensus sequence representing the entire JMRV genome. The sequencing redundancy achieved with this approach was ~6-fold. As sequenced, the JMRV genome is 131,217 bp in length, and restriction digestion of purified viral DNA confirmed the overall organization and structure of the determined genomic sequence (Table 1 and Fig. 1). In addition, CLUSTAL W alignment of the complete genomic sequences of JMRV and RRV_{17577} indicates that these viruses share 89.5% identity at the nucleotide level. The complete genomic sequence of JMRV is available in GenBank under accession number AY528864.

Structurally, the JMRV genome is similar to that of other gammaherpesviruses, possessing a linear double-stranded DNA genome comprised of a single long unique region (LUR) flanked by terminal repeat (TR) sequences at the genome termini (Fig. 2). Partial TR sequences were initially identified at both ends of the genome based on the presence of a series of identical repetitive tandem repeat sequences near the genome termini. The sequence of the complete TR was also determined and is described in more

TABLE 1 Restriction fragments of the JMRV genome

Restriction fragment	Size (bp)[a]	Nucleotide positions
HindIII	28,873	82234–111106
	23,773	137–23909
	18,781	111107–129887
	9,867	39334–49200
	9,511	49201–58711
	6,912	74047–80958
	6,348	32133–38480
	4,883	69164–74046
	4,750	23910–28659
	4,624	58712–63335
	3,473	28660–32132
	2,552	66201–68752
	2,463	63738–66200
	1,275	80959–82233
	853	38481–39333
	755	129888–130642
	575*	130643–131217
	411	68753–69163
	402	63336–63737
	136*	1–136
BamHI	22,949	20762–43710
	15,460	96218–111677
	11,194	9568–20761
	10,544	85477–96020
	9,986*	121232–131217
	9,748	43711–53458
	9,567*	1–9567
	7,320	76430–83749
	7,137	53459–60595
	5,836	63607–69442
	5,136	71294–76429
	4,466	115052–119517
	3,374	111678–115051
	3,011	60596–63606
	1,851	69443–71293
	1,727	83750–85476
	1,627	119518–121144
	197	96021–96217
	87	121145–121231

[a] *, Fragments linked to a variable number of terminal repeat sequences.

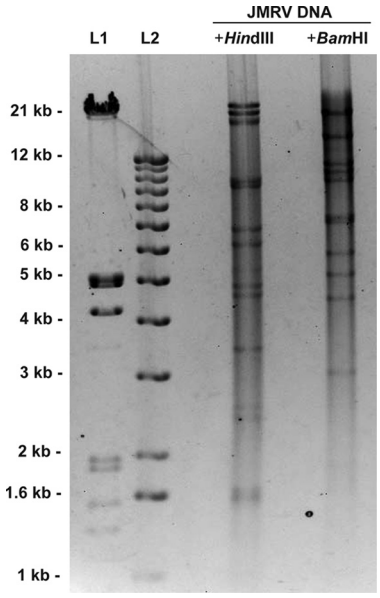

FIG 1 Restriction digest analysis of JMRV DNA. A 2.5-μg portion of purified viral genomic DNA was digested overnight with HindIII or BamHI and run on a 0.7% agarose gel. The patterns obtained for both digestions correlate with the predicted fragment sizes for the JMRV genomic sequence, as listed in Table 1. L1 and L2 represent DNA ladders run as size standards.

detail below. When excluding the partial TR sequences, the LUR spans nucleotides (nt) 907 to 129986 of the JMRV sequence. The overall G+C content of the JMRV LUR is 51.6%, which is less than the 52.2% G+C content of the RRV LUR and the 53.5% G+C content of the HHV-8 LUR (6).

Internal repeat sequences were identified in the LUR of JMRV, with a majority being similar in size, structure, and location to the repeat in divergent loci (rDL) that were previously identified in RRV_{17577}. The repeat regions identified in JMRV that possess similarity to those in RRV were thus designated with similar nomenclature as rDL-B 1 and 2, rDL-E 1 and 2, and rDL-F. Only one internal repeat was identified in JMRV (designated Repeat 1) that does not appear to have a counterpart in RRV and consists of four repeat elements in tandem from nt 21026 to 21121. The sequences, sizes, and locations of all of the identified internal JMRV repeats are presented in Table 2. As is the case in other herpesviruses, the actual number of repeat elements present within each repeat region is also likely somewhat variable within individual viral genomes, reflecting the fluctuating nature of the size of these regions during replication.

Identification of JMRV TRs. The observation of identical repeated sequences at the termini of the JMRV genome suggested an apparent duplication in these regions that were both likely to represent at least a portion of a TR unit. Further, the presence of a unique HindIII site within the repeated sequence at both ends of the genome indicated that it might be possible to isolate and identify the complete TR unit via restriction digestion analysis with this enzyme. Indeed, when viral DNA was subjected to digestion with HindIII, the resulting pattern indicated the presence of an ~1.6-kb restriction fragment (Fig. 3A), which is not a fragment size predicted to be generated by digestion with this enzyme (Table 1). Importantly, the intensity of this band was also stronger than other low-molecular-weight bands of similar size produced by HindIII digestion, suggesting that this sequence is likely overrepresented in the viral genome, and thus, may be derived from multiple copies of the TR unit present in the viral genome. This

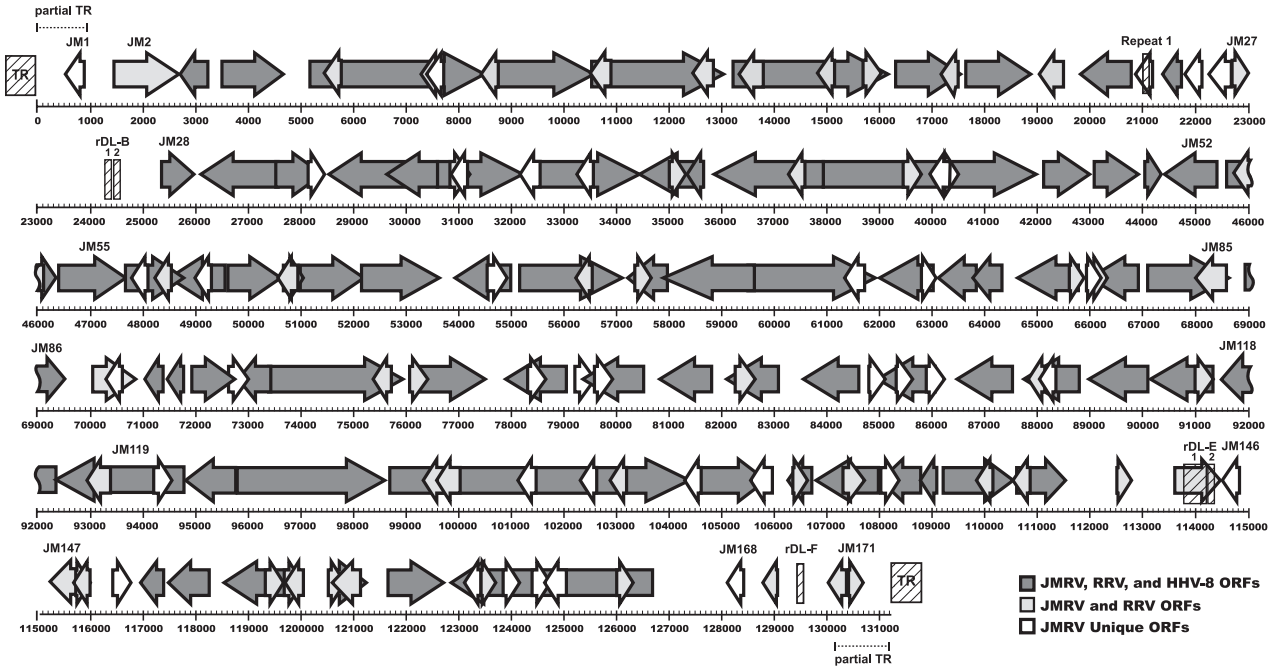

FIG 2 Map of the JMRV genome. All predicted JMRV ORFs are depicted by arrows, and the scale (in base pairs) indicates their approximate genomic location. ORFs are numbered from left to right as described in Table 3, with only selected ORFs labeled for purposes of clarity. JMRV ORFs that are homologous to RRV ORFs are shaded light gray, those homologous to both RRV and HHV-8 ORFs are shaded dark gray, and those unique to JMRV are white. Internal repeat regions are indicated by hashed boxes and are labeled with the corresponding repeat name above their location. Hashed boxes at the ends of the genome depict the location of TRs, and dashed lines at the genome termini indicate the approximate location of the partial TR sequences.

TABLE 2 JMRV repeat sequences[a]

JMRV repeat	Genomic position (nt)	Element size (no. of nt)	Sequence	No. of copies	RRV counterpart	%G+C
Repeat 1	21026–21121	24	GGCGTCTCCCCCGGAGTCTCCCCC	4	None	79.2
rDL-B 1	24250–24483	26	TAGCTCCTAATGTTTGCCTTGCCGCC	9	rDL-B 1	53.8
rDL-B 2	24649–25098	25	CGTTCCCCGAGGGTCCCGGTCTCCC	18	rDL-B 2	78.0
rDL-E 1	113629–114236	19	GTGCAGGTCCCCCGGTGGG	32	rDL-E 1	79.0
rDL-E 2	114237–114320	28	GCTCCGGGTGGCTCCGGGTGGGGTGGCG	3	rDL-E 2	82.1
rDL-F	129459–129590	22	AGCTAGGGTGAGGGCTGGGGTG	6	rDL-F	68.2

[a] nt, nucleotides.

observation is similar to that made during the identification of the HHV-8 TR (7).

To determine the sequence of the 1.6-kb HindIII fragment, the corresponding band was isolated from an agarose gel, purified, cloned into vector pSP73, and a clone containing the fragment was then isolated and subjected to sequence analysis. The digestion product was identified as a 1,564-bp HindIII fragment with a G+C content of 75%, and structural features similar to those found in other herpesvirus TR sequences (8). The precise order of the sequence of the TR unit was further defined based on the partial TR sequences present at both ends of the genome (Fig. 3B). Importantly, the TR of JMRV possesses sequences that have homology to herpesvirus *pac-1* (C_n-G_n-T motif-G_n) and *pac-2* (N_n-T_n-N_n) motifs, which are conserved sequences involved in directing the cleavage and packaging of head-to-tail viral genome concatemers (9). As in other herpesviruses, the TR sequence is bordered on the left side by a *pac-1* motif, and the right side by a *pac-2* motif. Tandem direct repeat (DR) sequences also exist within the TR, with the first repeat unit, direct repeat 1 (DR1), being composed of 12mer (GGCCTGCTTGCT). The observed number of DR1 varies in number from 24 (left partial TR) to 26 (right partial TR) in the genomic sequence and is present in 25 copies in the cloned TR fragment. The DR1 sequences are followed by a 35mer repeat unit (GCCTGCTTGCTTGCTGCTGAG GGGACAGTAGGGCT), termed direct repeat 2 (DR2), with the first repeat unit overlapping with the last DR1 unit present in the TR sequence. Three tandem copies of the DR2 unit were observed in both partial TRs in the genomic sequence, as well as the cloned TR sequence.

Based on the complete TR unit sequence and on the partial TR sequences present at the genome termini, the true LUR of JMRV was determined to span nt 907 to 129985 of the genomic sequence, with partial TR sequences located from nt 1 to 906 at the left end of the genome and from nt 129986 to 131217 at the right end of the genome. The partial TR identified at the left end of the genome consists of the last 906 bp of a complete TR unit and thus may simply represent an incompletely sequenced but fully intact TR, whereas the partial TR at the right end of the genome actually lacks the first 208 bp of the TR unit sequence and therefore represents an incomplete TR directly adjacent to the LUR. Although the genome termini as sequenced only possess partial fragments of the TR at their ends, they are likely to extend further into the TR unit sequence and also be flanked by an unknown number of multiple copies of the TR in tandem (Fig. 3C). It is unclear at this point exactly how many tandem copies of the 1,564-bp TR unit are typically present at the ends of the viral genome, although based on predictions made for gammaherpesviruses HVS and HHV-8 (7, 10), JMRV is likely to possess a relatively fixed overall number of ~35 total TRs per genome, with the exact number of TRs located at each end of the JMRV genome varying between different molecules.

JMRV ORF analysis. The target search criterion for identification of ORFs in the viral genome were set for sequences predicted to encode proteins of 80 aa or more. Putative ORFs identified in this fashion were translated, and homologous proteins were identified using BLASTP with standard settings. Genes are numbered from left to right starting with the first predicted ORF in the genomic sequence, and the JM prefix precedes each gene number. The arrangement of JMRV genes is shown in Fig. 2.

After identification of the ORFs in JMRV, a phylogenetic analysis was performed by bootstrap analysis using protein sequences for the DNA polymerase from JMRV and several gammaherpesviruses, including HHV-8, RRV, HVS, rhesus lymphocryptovirus, MHV-68, and EBV. The results of this analysis confirm that JMRV is a gammaherpesvirus most closely related to HHV-8 and RRV (Fig. 4). Indeed, the ORFs shared between these viruses are arranged collinearly (6, 11–13), and of the 171 predicted ORFs in JMRV, 88 encode proteins that are homologous to known or predicted proteins that were previously identified in RRV (6, 14). The highest level of identity observed between JMRV and RRV proteins is 99% (RRV ORF25, ORF26, ORF39, ORF49, ORF55, and ORF62), while the lowest is 48% (RU4-R) (Table 3).

Eighty-three small ORFs that encode putative proteins of ≥80 aa were also identified in JMRV. Predicted proteins of similar size were not previously identified in RRV, since this is less than the cutoff level that was utilized during the initial characterization of RRV (6). Thus, to determine whether any of these ORFs are specific to JMRV, the RRV genome was reanalyzed to include ORFs that would encode proteins of ≥80 aa. From this analysis it was determined that 44 of the small JMRV ORFs are also predicted to be present in the RRV genome (denoted in Table 3 as unnamed ORFs based on the nucleotide position in RRV), while 39 are unique to JMRV. The function of the proteins predicted to be encoded by the 39 JMRV-specific ORFs remains unknown, and BLAST analysis does not suggest any readily apparent homology to any known proteins. However, due to the presence of these unique ORFs in JMRV, and their absence in RRV, it is possible that some of these ORFs may encode proteins that confer unique pathogenic qualities to JMRV. These ORFs are being examined in further detail to determine their potential functions.

Interestingly, several ORFs are predicted to be present in locations of the genome containing repeat sequences. For example, JM145 spans the region containing rDL-E 1 and 2, while Repeat 1 is located within JM23. If these regions are in fact capable of producing functional transcripts and supporting protein expression, these ORFs could produce variable proteins depending on the

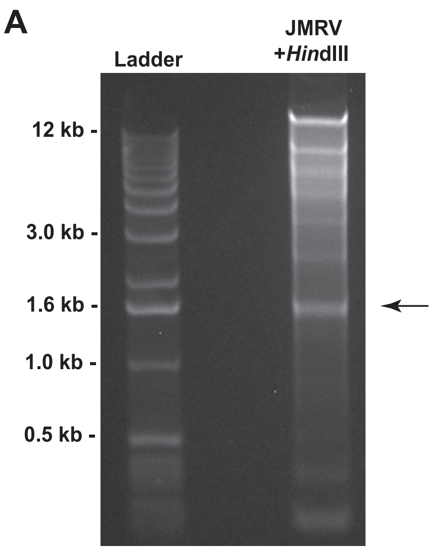

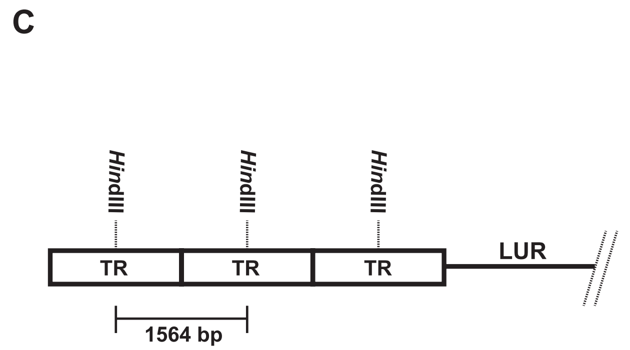

B

```
1                                          pac-1                                          100
CCCGACTCGCGCGAAACCCGGGGGACGGGGCGACTCGCGCGAAACCCCCCGGGGGGTATTTTAGGGGGGGGGTACTTTTTGCCCGTGCCCCCTCGGCCCC

101                                                                                       200
TTGACACAACGTCCACCAGTGTCCCCCAAGCACCGTCCACCACCAGTGTCCCCCCACGCTCACACGCCTCCCCTCCCCCGCCCGGGCGCCGGCCGCATCT
                                                             JM170-TR Stop
201      *                                                                                300
GGCGGTCTGCGAGGGCCCCTAGCGGCGGCGCCCGGCGGGGGCCCCCAGGCGCCCGGCCGGCGGCGGCGCGGGGCCGCGGCCGCCATCTTGCGCCCGGGGC

301                                                                                       400
GAGGGTCTCCCGCGCGGCCCCCGGGCCCCCGAGCGGGGCGCCGCCGGCCTCCCCCGGCTCCCGGCCCTCCGCCCGGCCGGCCCGGGCCCGCGGCCGCCGC

401                                                                                       500
CCCCGGCCGCCCCGCGCCGCGCGCCGGGCCGCTTTCGGTTCGCGGGGCCGGGGGTCCCGCGGGGGGCCGGGGCCGCCCCCGGGTCCCGCTCCGCCGGGCC

501                                                                                       600
CCGCCGACTCCCGGGAGCGCCCCGGTCCGGCCGAGCCCGGCGGCGCCGCGCCCCGACGCCCCCCGAGCCCGGGGCCCCACAAGCCGCGGCGCGCGGCTCC

601 JM171 Start                                                                           700
CGATGCCGGGCGGCCGCCGCCCGGCATGGCGGTCCTCCGCCGGCCTCCCCTCCCCCACGTCGCCCCGAAAGGTGGTCTCCGCGCCGCCGGGAGGGGGGCT
          JM170-TR Start
701                                                                                       800
GGGGCCCGGGGCGCCTCGGCGGGGCCGGCCCCGGGGCGCGACCGAGGGCCCCGGGAGAACGGGGGATCGGGAAAACGCGAGGGGTGGCGGGGGACAGAGG

801                                                               HindIII  JM171 Stop     900
GGAACGTGTGCGTGCTTGTGGAACACTATGGCCTGCTGGCCTGCTCGCTTGCTTGGTAGCTTGCAAGCTTGCTGCTGAGAGACTTTAGAGGGACAGTAGG

901                                               DR1                                     1000
CCTGCTTGCTGGCCTGCTTGCTGGCCTGCTTGCTGGCCTGCTTGCTGGCCTGCTTGCTGGCCTGCTTGCTGGCCTGCTTGCTGGCCTGCTTGCTGGCCTG

1001                                                                                      1100
CTTGCTGGCCTGCTTGCTGGCCTGCTTGCTGGCCTGCTTGCTGGCCTGCTTGCTGGCCTGCTTGCTGGCCTGCTTGCTGGCCTGCTTGCTGGCCTGCTTG

1101                                                             DR2                      1200
CTGGCCTGCTTGCTGGCCTGCTTGCTTGCTGCTGAGGGGACAGTAGGGCTGCCTGCTTGCTTGCTGCTGAGGGGACAGTAGGGCTGCCTGCTTGCTTGCT

1201                                                                                      1300
GCTGAGGGGACAGTAGGGCTGCCTGCTTGCTTGCTGCTGAGTAGGACTGCTAGGGCTGGTAGTAGTGGGGCAGCCGGCCAGCTGCGTGCGAGGGCGTTGC
                                                 JM1 Stop
1301                                                                                      1400
AGGGCCACACGAGGACACGGGACCCGAGCCCTCCCCAGGACCGCCGGGCAAGCGGCCCAGATCTGCCCGGCAGGTCGCTCGGGGAGAGCGGACGGAAAGG

1401                                                                                      1500
GCGGTGGGGGCTGGGAGCATAGACGCGGGGCTGGGAACGGGGAGTAGGGGGATGGGAAGGGGTGCAGACGTGGGGCCGGGGGACGGGGCGTGGTTTGAGA

1501                                        pac-2
CCCCAAGCTGATGACTCAAAAATGGGCTAAACCACGCCCACCTCATTTTTTTCCCCCGGCCC
                                       JM1 Start
```

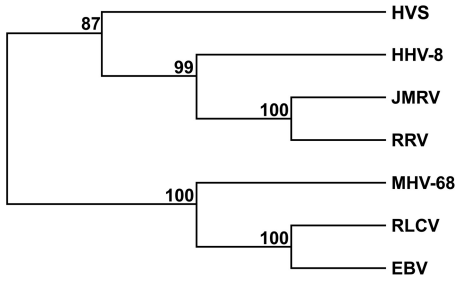

FIG 4 Phylogenetic tree of selected gammaherpesviruses. The protein sequence of DNA polymerase from JMRV, RRV, HHV-8, HVS, RLCV, MHV-68, and EBV were subjected to bootstrap analysis (1,000 replicates) using the neighbor joining method. Numbers represent the percentage of bootstrap trees that contain the same branch point.

exact structure of the repeats within a given virus. Further, examination of the TR unit sequence indicates the presence of two complete predicted ORFs that are also contained within the partial TR sequences at the left and right end of the sequenced genome (JM1 and JM171, respectively), as well as a variant of JM170.

As the last predicted ORF at the right end of the genome, JM170 actually overlaps the junction of the LUR and the partial TR sequence located at the genome terminus. Thus, while the form of JM170 found within the complete TR unit contains a nearly full duplication of JM170 sequence, it varies in that the last 16 bp of the 435-bp JM170 ORF are replaced with a different 49-bp sequence. Due to this difference, this ORF has been denoted as JM170-TR. If JM170-TR is indeed transcribed and expressed from the TR, it would result in the production of a protein in which the C-terminal 4 aa of the predicted 144-aa JM170 protein are replaced with a different 15-aa sequence. Therefore, JM170-TR may represent a variant of JM170 that is strictly expressed from the TR unit.

The apparent duplication of portions of the viral genome as parts of the TR results in the possibility that viral genes contained within this sequence may actually be present in multiple copies in the virus due to amplification of the TR. This suggests that viral genes present within the TR of JMRV that are capable of being transcribed and expressed might be present in abundance in infected cells. A similar observation has been made in MHV-68, which also contains predicted ORFs within the TR (15). However, the putative functions of all three proteins encoded by the ORFs located in the JMRV TR are currently unknown and, based on database searches, none appear to share strong sequence homology to any known proteins. Regardless, it will be important to determine whether or not these genes are highly expressed during infection and, if so, what impact(s) they may potentially have on viral disease.

Expression of JMRV-unique genes during infection. To address whether any predicted unique JMRV ORFs are actually expressed during JMRV infection, analysis was undertaken to identify transcripts produced by a selection of these ORFs. Specifically, four JMRV-unique ORFs were examined; JM1, JM25, JM150, and JM168, which are predicted to encode small proteins of 10, 9.8, 10.2, and 14 kDa, respectively. These ORFs were chosen since they are located in distinct regions of the genome and are do not overlap with any other predicted JMRV ORFs. In addition, one of these ORFs, JM1, is located within the TR unit of JMRV and thus represents a gene with the potential to be present in multiple copies within infected cells. To determine whether these genes are actually expressed during JMRV infection and also to attempt to define their kinetic class, transcriptional analysis was undertaken using RNA isolated from JMRV-infected primary rhesus fibroblasts. Briefly, cells were infected with JMRV and treated with cycloheximide (CHX) to inhibit protein synthesis, ganciclovir (GCV) to inhibit DNA replication, or left untreated to define transcripts as immediate-early, early, or late, respectively. The time points for collection of RNA were 24 h (+CHX), 48 h (+GCV), and 72 h (untreated). RNA from mock-infected cells collected at 72 h served as a negative control for all reactions. The isolated RNA was then used in RT-PCR with primers specific to each ORF, and the results from this analysis demonstrated that transcripts associated with all four predicted ORFs are produced in JMRV-infected cells (Fig. 5). In regard to the kinetics of their expression, JM1 is expressed as an early gene, JM25 is an early gene with some leaky immediate-early expression, JM150 is a late gene with some leaky early expression, and JM168 is a strict late gene.

Despite the fact that the predicted proteins encoded by these ORFs do not appear to possess significant homology to any known proteins, and their potential functions currently remain unknown, given their small sizes it is possible that they represent secreted proteins that are somehow involved in pathogenesis. Although analysis of the protein sequences encoded by these ORFs for possible secretory motifs does not reveal the presence of classical signal peptides, nonclassical secretion signals are predicted to exist for JM1, JM25, and JM150 (data not shown). Further characterization of these genes is ongoing to determine their exact functions and assess what roles they may play in the development of JMRV-associated disease.

Deep sequencing analysis of JMRV plaque isolates. In addition to the original stock of JMRV, which likely represents a swarm of strain variants, two plaque-purified isolates of JMRV were also obtained. These viruses were designated isolates 3A1 and 12E2. Both plaque isolates were examined by *in vitro* growth analysis and found to replicate with similar kinetics to the parental virus (data not shown). To compare the genomic sequence of these plaque isolates, genomic DNA was purified from each virus, and deep sequencing analysis of the complete genome of each isolate was performed. After assembly of the individual reads from the deep sequencing analysis into contiguous sequences, a consensus se-

FIG 3 Identification of the TR sequence. (A) Purified viral DNA was digested with HindIII and run on a 1% agarose gel, resulting in the identification of an ~1.6-kb digestion product corresponding to the terminal repeat (TR) unit of JMRV. This fragment was purified, cloned, and sequenced. (B) The TR unit of JMRV is 1,564 bp in length and possesses defining features of a herpesvirus TR, including the presence of direct repeats (DR1 and DR2) and packaging motifs (*pac-1* and *pac-2*). The TR also possesses three potential ORFs: JM1, JM171, and JM170-TR. JM170-TR is a variant of JM170 that possesses an alternate 49 nt at its 3′ end. The alternate 49-nt sequence of JM170-TR is denoted in the TR sequence by italicized lettering, and the location of the junction of the LUR and partial TR located at the right end of the genome is marked by an asterisk. (C) Diagram depicting the predicted layout of TR units at the termini of the JMRV genome. The size marker indicates the fragment produced by HindIII digestion of viral DNA, in relation to the orientation of the TR units. The exact number of copies of the TR at the ends of the genome is unknown and varies between individual viral genomes.

TABLE 3 Predicted JMRV ORFs[a]

JMRV ORF	First nt	Last nt	Coding strand[b]	Size (aa)	Putative function[c]	RRV ORF homologue (nt position)[d]	Homologue size (no. of aa)	% Identity of overlap[e]
JM001	**890**	**594**	**–**	**98**	**Unknown**	**None**		
JM002	1444	2721	+	425	Signal transduction, transformation	R1	423	85
JM003	3359	2778	–	193	Dihydrofolate reductase	ORF2	188	95
JM004	3526	4713	+	395	Complement regulatory protein	ORF4	645	56
JM005	5146	8544	+	1132	ssDNA binding protein	ORF6	1,132	98
JM006	5895	5581	–	104	Unknown	Unnamed (6480–6794)	104	83
JM007	7676	7410	–	88	Unknown	Unnamed (8309–8575)	88	94
JM008	**7722**	**7462**	**–**	**86**	**Unknown**	**None**		
JM009	8792	8541	–	83	Unknown	Unnamed (9440–9691)	83	91
JM010	8569	10629	+	686	DNA packaging protein	ORF7	686	97
JM011	10929	10606	–	107	Unknown	Unnamed (11436–11828)	130	94
JM012	10616	13102	+	828	Glycoprotein B	ORF8	829	96
JM013	12858	12565	–	97	Unknown	Unnamed (13467–13760)	97	97
JM014	13219	16257	+	1012	DNA polymerase catalytic subunit	ORF9	1014	97
JM015	13827	13267	–	186	Unknown	Unnamed (14170–14736)	188	85
JM016	15117	14809	–	102	Unknown	Unnamed (15646–16026)	126	92
JM017	15726	16031	+	101	Unknown	Unnamed (16635–16940)	101	88
JM018	16351	17601	+	416	Unknown	ORF10	384	95
JM019	17501	17226	–	91	Unknown	Unnamed (18136–18411)	91	94
JM020	17610	18839	+	409	Unknown	ORF11	409	98
JM021	19641	19018	–	207	Viral IL-6	R2	207	91
JM022	20862	19861	–	333	Thymidylate synthase	ORF70	333	93
JM023	**21235**	**20969**	**–**	**88**	**Unknown**	**None**		
JM024	21748	21386	–	120	Viral macrophage inflammatory protein	R3	115	74
JM025	**22120**	**21845**	**–**	**91**	**Unknown**	**None**		
JM026	**22701**	**22363**	**–**	**112**	**Unknown**	**None**		
JM027	22700	23008	+	102	Unknown	RU1-R	102	74
JM028	25392	25955	+	187	viral Bcl-2	ORF16	187	96
JM029	27672	26062	–	536	Capsid protein	ORF17	536	94
JM030	27545	28444	+	299	Unknown	ORF18	299	97
JM031	**28138**	**28431**	**+**	**97**	**Unknown**	**None**		
JM032	30095	28452	–	547	Tegument protein	ORF19	547	97
JM033	30642	29590	–	350	Unknown	ORF20	350	91
JM034	30641	32311	+	556	Thymidine kinase	ORF21	557	97
JM035	30825	31181	+	118	Unknown	Unnamed (32278–32637)	119	87
JM036	**31111**	**30863**	**–**	**82**	**Unknown**	**None**		
JM037	**32608**	**32279**	**–**	**109**	**Unknown**	**None**		
JM038	32298	34478	+	726	Glycoprotein H	ORF22	704	75
JM039	**33553**	**33254**	**–**	**99**	**Unknown**	**None**		
JM040	35038	34475	–	187	Unknown	ORF23	402	96
JM041	34974	35285	+	103	Unknown	Unnamed (36427–36828)	134	89
JM042	35687	35301	–	128	Unknown	ORF23	402	95
JM043	37938	35737	–	733	Unknown	ORF24	732	97
JM044	37612	37346	–	88	Unknown	Unnamed (38732–38998)	88	88
JM045	37937	42073	+	1378	Major capsid protein	ORF25	1,378	99
JM046	39498	39821	+	107	Unknown	Unnamed (40884–41207)	107	87
JM047	**40282**	**39842**	**–**	**146**	**Unknown**	**None**		
JM048	**40188**	**40439**	**+**	**83**	**Unknown**	**None**		
JM049	42105	43022	+	305	Capsid protein	ORF26	305	99
JM050	43047	43871	+	274	Unknown	ORF27	269	91
JM051	44035	44310	+	91	Unknown	ORF28	91	91
JM052	45406	44360	–	348	DNA packaging protein	ORF29b	348	98
JM053	45720	46373	+	217	Unknown	ORF31	217	96
JM054	46195	45836	–	119	Unknown	Unnamed (47209–47568)	119	93
JM055	46310	47695	+	461	DNA packaging protein	ORF32	464	95
JM056	47676	48686	+	336	Tegument protein	ORF33	336	91
JM057	**48136**	**47768**	**–**	**122**	**Unknown**	**None**		

(Continued on following page)

TABLE 3 (Continued)

JMRV ORF	First nt	Last nt	Coding strand[b]	Size (aa)	Putative function[c]	RRV ORF homologue (nt position)[d]	Homologue size (no. of aa)	% Identity of overlap[e]
JM058	48607	48218	–	129	Unknown	Unnamed (49066–50040)	324	87
JM059	49587	48604	–	327	DNA packaging protein	ORF29a	327	97
JM060	**49276**	**49010**	**–**	**88**	**Unknown**	**None**		
JM061	49586	50572	+	328	Unknown	ORF34	327	95
JM062	50950	50504	–	148	Unknown	Unnamed (51874–52413)	179	94
JM063	50553	51002	+	149	Unknown	ORF35	149	95
JM064	50908	52215	+	435	Serine/threonine protein kinase	ORF36	435	96
JM065	52196	53638	+	480	Alkaline exonuclease	ORF37	480	97
JM066	55018	53882	–	378	Glycoprotein M	ORF39	378	99
JM067	54536	54850	+	104	Unknown	None		
JM068	55153	57156	+	667	DNA helicase/primase complex	ORF40	468	96
JM069	56474	56124	–	116	Unknown	Unnamed (57497–57847)	116	96
JM070	57968	57153	–	271	Unknown	ORF42	272	95
JM071	57325	57573	+	82	Unknown	Unnamed (58700–58948)	82	97
JM072	59652	57907	–	581	Capsid protein	ORF43	576	98
JM073	59591	61963	+	790	Helicase/primase complex	ORF44	790	98
JM074	**61662**	**61249**	**–**	**137**	**Unknown**	**None**		
JM075	63065	62004	–	353	Immediate-early phase viral replication	ORF45	352	90
JM076	**62823**	**63086**	**+**	**87**	**Unknown**	**None**		
JM077	63874	63107	–	255	Uracil-DNA glycosylase	ORF46	255	91
JM078	64341	63850	–	163	Glycoprotein L	ORF47	169	55
JM079	65769	64600	–	389	Unknown	ORF48	389	92
JM080	65629	65880	+	83	Unknown	Unnamed (67028–67279)	83	96
JM081	**65963**	**66208**	**+**	**81**	**Unknown**	**None**		
JM082	66905	66000	–	301	Unknown	ORF49	301	99
JM083	66058	66315	+	85	Unknown	Unnamed (67456–67713)	85	97
JM084	67096	68640	+	514	Replication and transcription activator	ORF50	514	95
JM085	68594	67920	–	224	Unknown	Unnamed (69312–69956)	214	88
JM086	68957	69469	+	170	bZIP transcription factor	ORF51	161	83
JM087	70026	70760	+	244	Glycoprotein	Glycoprotein R8.1	230	90
JM088	70606	70328	–	92	Unknown	Unnamed (71728–71970)	80	89
JM089	71420	71001	–	139	Unknown	ORF52	139	96
JM090	71797	71483	–	104	Envelope glycoprotein	ORF53	104	98
JM091	71873	72745	+	290	dUTPase	ORF54	290	98
JM092	**72520**	**72942**	**+**	**140**	**Unknown**	**None**		
JM093	73438	72806	–	210	Unknown	ORF55	210	99
JM094	73420	75936	+	838	Helicase/primase complex	ORF56	828	97
JM095	75722	75447	–	91	Unknown	Unnamed (76848–77123)	91	96
JM096	76035	76304	+	89	Unknown	Unnamed (77451–77753)	100	80
JM097	76162	77484	+	440	Immediate-early phosphoprotein	ORF57	442	93
JM098	79098	77857	–	413	vIRF	R6	415	87
JM099	**78411**	**78656**	**+**	**81**	**Unknown**	**None**		
JM100	**79163**	**79579**	**+**	**138**	**Unknown**	**None**		
JM101	80510	79269	–	413	vIRF	R7	415	91
JM102	**79521**	**79796**	**+**	**91**	**Unknown**	**None**		
JM103	81891	80836	–	351	vIRF	R8	351	93
JM104	83153	82068	–	361	vIRF	R9	253	95
JM105	82206	82613	+	135	Unknown	Unnamed (83629–84111)	160	82
JM106	84785	83628	–	385	vIRF	R10	385	86
JM107	**84837**	**85082**	**+**	**81**	**Unknown**	**None**		
JM108	86104	84932	–	390	vIRF	R11	390	83
JM109	**85290**	**85550**	**+**	**86**	**Unknown**	**None**		
JM110	**85968**	**86243**	**+**	**91**	**Unknown**	**None**		
JM111	87546	86479	–	355	vIRF	R12	355	88
JM112	88801	87707	–	364	vIRF	R13	364	87
JM113	88023	87763	–	86	Unknown	Unnamed (89178–89438)	86	76

(Continued on following page)

TABLE 3 (Continued)

JMRV ORF	First nt	Last nt	Coding strand[b]	Size (aa)	Putative function[c]	RRV ORF homologue (nt position)[d]	Homologue size (no. of aa)	% Identity of overlap[e]
JM114	**88395**	**88087**	**–**	**102**	**Unknown**	**None**		
JM115	90129	89047	–	360	Unknown	ORF58	360	96
JM116	91324	90140	–	394	DNA replication protein	ORF59	394	97
JM117	91017	91259	+	80	Unknown	Unnamed (92432–92674)	80	97
JM118	92399	91455	–	314	Ribonucleotide reductase small subunit	ORF60	314	98
JM119	94747	92381	–	788	Ribonucleotide reductase large subunit	ORF61	788	97
JM120	93345	92929	–	138	Unknown	Unnamed (94342–94758)	138	92
JM121	**94175**	**94468**	**+**	**97**	**Unknown**	**None**		
JM122	95746	94751	–	331	Assembly/DNA maturation protein	ORF62	331	99
JM123	95745	98564	+	939	Tegument protein	ORF63	939	96
JM124	98568	104468	+	1966	Tegument protein	ORF64	2,548	96
JM125	99753	99388	–	121	Unknown	Unnamed (100644–101165)	173	93
JM126	100054	99611	–	147	Unknown	Unnamed (101023–101466)	147	95
JM127	**101428**	**101108**	**–**	**106**	**Unknown**	**None**		
JM128	**102568**	**102290**	**–**	**92**	**Unknown**	**None**		
JM129	103150	102857	–	97	Unknown	Unnamed (104269–104562)	97	91
JM130	**104643**	**104302**	**–**	**113**	**Unknown**	**None**		
JM131	104555	105856	+	433	Tegument protein	ORF64	2,548	88
JM132	**106003**	**105581**	**–**	**140**	**Unknown**	**None**		
JM133	106729	106220	–	169	Capsid protein	ORF65	169	98
JM134	106299	106559	+	86	Unknown	Unnamed (107716–107976)	86	95
JM135	108079	106733	–	448	Unknown	ORF66	448	92
JM136	107289	107696	+	135	Unknown	Unnamed (108708–109040)	110	84
JM137	108780	107974	–	268	Tegument protein	ORF67	224	98
JM138	**108002**	**108316**	**+**	**104**	**Unknown**	**None**		
JM139	109056	108796	–	86	DNA packaging protein	ORF67.5	86	95
JM140	109190	110563	+	457	Glycoprotein	ORF68	457	95
JM141	110166	109783	–	127	Unknown	Unnamed (111202–111585)	127	90
JM142	110904	110578	–	108	Unknown	Unnamed (111979–112323)	114	95
JM143	110585	111478	+	297	Capsid maturation protein	ORF69	297	97
JM144	112447	112698	+	83	Unknown	RU3-R	101	69
JM145	113610	114479	+	289	Unknown	RU4-R	486	48
JM146	**114753**	**114427**	**–**	**108**	**Unknown**	**None**		
JM147	115918	115214	–	234	Unknown	RU13-L	151	65
JM148	**115671**	**115928**	**+**	**85**	**Unknown**	**None**		
JM149	115983	115717	–	88	Unknown	RU13-L	151	92
JM150	**116366**	**116650**	**+**	**94**	**Unknown**	**None**		
JM151	117442	116918	–	174	v-FLIP	ORF71	174	91
JM152	118265	117501	–	254	Cyclin D	ORF72	254	93
JM153	119918	118608	–	436	Latency-associated nuclear antigen	ORF73	448	86
JM154	119237	119617	+	126	Unknown	Unnamed (121540–121920)	126	87
JM155	119614	119940	+	108	Unknown	Unnamed (121917–122234)	105	73
JM156	120075	119824	–	83	Unknown	Unnamed (122118–122369)	83	96
JM157	120484	120744	+	86	Unknown	Unnamed (122778–123038)	86	91
JM158	120572	121333	+	253	CD200 homologue	R15	253	97

(Continued on following page)

TABLE 3 (Continued)

JMRV ORF	First nt	Last nt	Coding strand[b]	Size (aa)	Putative function[c]	RRV ORF homologue (nt position)[d]	Homologue size (no. of aa)	% Identity of overlap[e]
JM159	121186	120689	–	165	Unknown	Unnamed (122983–123480)	165	90
JM160	121628	122656	+	342	G protein-coupled receptor	ORF74	342	96
JM161	126658	122762	–	1298	FGARAT/tegument protein	ORF75	1,298	95
JM162	**123398**	**123126**	**–**	**90**	**Unknown**	**None**		
JM163	123423	123677	+	84	Unknown	Unnamed (125718–125972)	84	88
JM164	**123810**	**124133**	**+**	**107**	**Unknown**	**None**		
JM165	**124395**	**124790**	**+**	**131**	**Unknown**	**None**		
JM166	**125165**	**124683**	**–**	**160**	**Unknown**	**None**		
JM167	126063	126371	+	102	Unknown	Unnamed (128358–128666)	102	90
JM168	**128493**	**128122**	**–**	**123**	**Unknown**	**None**		
JM169	129046	128789	–	85	Unknown	RK15 exon 1	81	42
JM170	130404	129970	–	144	Unknown	Unnamed (132318–132731)	137	90
JM171	130380	130655	+	91	Unknown	Unnamed (132707–133009)	100	76

[a] The data are highlighted as follows: JMRV ORFs with homology to previously predicted RRV ORFs (unshaded, normal typeface), JMRVORFs with homology to previously unidentified and unnamed RRV ORFs (gray shaded), and JMRV ORFs with no identifiable homolog in RRV (unshaded, boldface type). nt, nucleotide(s); aa, amino acid(s).
[b] +, Top strand; –, bottom strand.
[c] Based on the known and predicted functions of homologous proteins.
[d] Based on sequence homology to RRV ORFs.
[e] That is, the percent identity of overlapping regions of viral proteins.

quence for each virus was generated representing the complete genomic sequence of each isolate. Using this approach, a sequencing redundancy of ~300-fold was obtained for both genomes.

Upon alignment of all of the JMRV genome sequences, several regions in both of the plaque isolate genomes were initially found to have small gaps in sequence compared to the original parental JMRV genome. Specifically, nine gaps were identified in the LUR of the consensus sequence of each plaque isolate (Table 4), most of which were determined to be located in regions corresponding to internal repeat sequences, including rDL-B 1 and 2, rDL-E 1 and 2, and rDL-F. These gaps all represent regions incompletely assembled during the generation of a consensus sequence for each isolate, due to the size of the short sequence reads generated by this method of sequencing and the repetitive nature of sequences in these regions. In addition to the gaps in LUR sequence, the presence of the highly repetitive DR1 and DR2 units in the TR resulted in smaller portions of the partial TR sequences in the isolate genomes being assembled. Specifically, the partial TR sequence at the left and right end of each genome extends only as far as the beginning of DR2 and DR1, respectively.

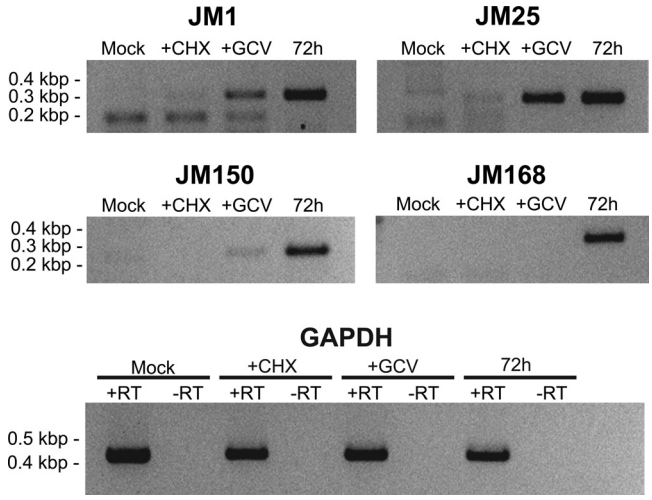

FIG 5 Analysis of JMRV-unique gene expression. RNA was purified from primary rhesus fibroblasts infected with JMRV and subjected to RT-PCR using primers specific for JMRV-unique ORFs. Cells were infected at an MOI of 5, treated with CHX, GCV, or left untreated, and collected at 24, 48, and 72 h, respectively. GAPDH (glyceraldehyde-3-phosphate dehydrogenase) reactions with RT (+RT) serve as controls for the presence of RNA, and GAPDH reactions without RT (−RT) demonstrate absence of DNA in each sample.

To confirm the identity of the gaps in LUR sequence of the plaque isolate genomes, PCR was performed using purified viral DNA from each respective plaque isolate and primer sets designed to amplify across these regions, followed by direct sequencing of the resulting products (Table 4). Only gaps 3 and 8 in the LUR of the plaque isolates, corresponding to rDL-B 2 and rDL-E 1/2, respectively, proved to be recalcitrant to complete PCR and sequencing across the entire region due to a combination of their highly repetitive nature and high GC content. The remaining gaps in the LUR sequences of the plaque isolates were all completely analyzed and confirmed to contain identical sequences to those identified in the parental JMRV genome, with only a few variances in repeat unit numbers detected in some locations. The nucleotide sequences of the plaque isolates were manually edited at locations confirmed by PCR and sequencing to reflect the presence of the sequences excluded from the original assemblies (Table 4). The sequences of both isolates are available in GenBank under accession numbers JN885136 (isolate 3A1) and JN885137 (isolate 12E2).

Based on nucleotide alignments of the complete genomic sequence of each virus (including the partial TR sequences), isolate

TABLE 4 Characterization of sequencing gaps[a]

Sequencing gap	Genomic location (nt)[b]		Gap size (bp)[c]		Edited genomic sequence (nt)[d]		Associated JMRV repeat
	3A1	12E2	3A1	12E2	3A1	12E2	
1	20493	20493	45	45	20493–20537	20493–20537	Repeat 1
2	23721	23721	170	196	23721–23890	23721–23916	rDL-B 1
3	24093	24119	ND	ND	NA	NA	rDL-B 2
4	26910	26936	35	35	26911–26945	26937–26971	
5	54754	54780	181	190	54755–54935	54781–54970	
6	82834	82860	110	110	82835–82944	82861–82970	
7	110918	110944	30	30	110919–110948	110945–110974	
8	112670	112696	ND	ND	NA	NA	rDL-E 1 and 2
9	127842	127868	92	92	127843–127934	127869–127960	rDL-F

[a] ND, not determined; NA, not applicable.
[b] That is, the first missing nucleotide in the gap.
[c] That is, the determined size of the missing sequence based on PCR analysis.
[d] That is, the location of the sequence confirmed by PCR and manually edited.

3A1 and 12E2 were found to be 100% identical to each other and 98.4% identical to the genomic sequence of the parental JMRV. Further, when only the LUR sequences of each genome were compared, isolates 3A1 and 12E2 were both found to be 99.2% identical to the parental JMRV genome sequence, with all of the observed differences between the parental and plaque isolate genomes being attributed to the lack of complete sequences across repeat regions rDL-B 2, rDL-E 1, and rDL-E 2 in the plaque isolates, as well as the presence of one ambiguous residue in isolate 3A1 and two ambiguous residues in isolate 12E2. Thus, both plaque isolates of JMRV represent clonal viruses derived from the parental JMRV strain, with which they share a high level of genetic identity.

DISCUSSION

JMRV was recently isolated from a JM that developed JME, a disease that possesses clinical and histopathological features that resemble MS in humans (1). As reported here, we have fully sequenced the complete genome of JMRV, as well as two plaque isolates of this virus, the results of which provide further evidence that JMRV is a gammaherpesvirus highly similar to other human and primate gammaherpesviruses. Specifically, JMRV is most closely related to RRV, a rhesus macaque herpesvirus that is associated with the development of lymphoproliferative disorders in simian immunodeficiency virus-infected rhesus macaques, as well as HHV-8, an oncogenic human herpesvirus (16, 17). Interestingly, JMRV is less closely related to EBV, a nearly ubiquitous human gammaherpesvirus that has been suggested to be associated in the development of MS (18). Despite these findings, it is possible that the genetic similarity of JMRV to human viruses such as EBV and HHV-8 is less important and may also suggest that an as-yet-unidentified gammaherpesvirus more closely related to JMRV, and potentially associated with MS, could also exist in humans.

JMRV possesses numerous unique ORFs not found even in closely related RRV, which may suggest these genes are important for the induction of virus-mediated disease in JMRV-infected animals. Examination of a selection of these predicted unique genes (JM1, JM25, JM150, and JM168) indicates that they are in fact expressed during JMRV infection *in vitro* and thus represent a potential source of novel viral protein products. One of these genes, JM1, is located within the TR unit and therefore likely to be present in multiple copies within the viral genome. Overrepresentation of JM1 in the viral genome could result in a high level of protein production from this gene during infection. Further analysis of these genes and their possible functions is ongoing.

In addition to unique genes, JMRV does share several ORFs with RRV that are of potential interest due to their predicted roles in immunoregulation and possible connections with inflammatory demyelinating disease development. These ORFs include JM21, JM24, and JM158, the homologues of RRV R2, R3, and R15, respectively. Although as yet functionally analyzed, JM21 encodes a viral homologue of interleukin-6, a cytokine that has been suggested to be linked to the development of MS (19); JM24 encodes a viral macrophage inflammatory protein (vMIP) that may be capable of affecting the infiltration of macrophages, a cell type which has been suggested to have a direct role in the development of MS lesions (20); and JM158 encodes a viral homologue of cellular CD200, a protein hypothesized to be critical for maintaining immune suppression in the brain that may also be dysregulated in MS patients (2, 21). Thus, it is possible that the expression of these viral genes in infected animals could induce immune alterations that ultimately result in the induction of JME.

Taken together, JMRV represents a novel and highly relevant model system for analyzing the possible role of an infectious agent in the development of inflammatory demyelinating disease. Due to the ability to easily propagate JMRV *in vitro* and the availability of the complete genomic sequence, identifying viral determinants of pathogenesis via molecular approaches may help shed significant light onto the role of specific viral genes in disease development.

ACKNOWLEDGMENTS

This study was supported by National Institutes of Health grants 8P51OD011092-53, CA075922 (S.W.W.), and CA132638 (S.W.W.) and U.S. Department of Defense grant W81XWH-09-1-0276 (S.W.W.).

REFERENCES

1. **Axthelm MK, Bourdette DN, Marracci GH, Su W, Mullaney ET, Manoharan M, Kohama SG, Pollaro J, Witkowski E, Wang P, Rooney WD, Sherman LS, Wong SW.** 2011. Japanese macaque encephalomyelitis: a spontaneous multiple sclerosis-like disease in a nonhuman primate. Ann. Neurol. **70**:362–373.
2. **Meuth SG, Simon OJ, Grimm A, Melzer N, Herrmann AM, Spitzer P, Landgraf P, Wiendl H.** 2008. CNS inflammation and neuronal degener-

ation is aggravated by impaired CD200-CD200R-mediated macrophage silencing. J. Neuroimmunol. **194**:62–69.
3. **Petersen TN, Brunak S, von Heijne G, Nielsen H.** 2011. SignalP 4.0: discriminating signal peptides from transmembrane regions. Nat. Methods **8**:785–786.
4. **Bendtsen JD, Jensen LJ, Blom N, Von Heijne G, Brunak S.** 2004. Feature-based prediction of non-classical and leaderless protein secretion. PEDS **17**:349–356.
5. **Hansen SG, Strelow LI, Franchi DC, Anders DG, Wong SW.** 2003. Complete sequence and genomic analysis of rhesus cytomegalovirus. J. Virol. **77**:6620–6636.
6. **Searles RP, Bergquam EP, Axthelm MK, Wong SW.** 1999. Sequence and genomic analysis of a Rhesus macaque rhadinovirus with similarity to Kaposi's sarcoma-associated herpesvirus/human herpesvirus 8. J. Virol. **73**:3040–3053.
7. **Lagunoff M, Ganem D.** 1997. The structure and coding organization of the genomic termini of Kaposi's sarcoma-associated herpesvirus. Virology **236**:147–154.
8. **Vink C, Beuken E, Bruggeman CA.** 1996. Structure of the rat cytomegalovirus genome termini. J. Virol. **70**:5221–5229.
9. **Deiss LP, Chou J, Frenkel N.** 1986. Functional domains within the a sequence involved in the cleavage-packaging of herpes simplex virus DNA. J. Virol. **59**:605–618.
10. **Bankier AT, Dietrich W, Baer R, Barrell BG, Colbere-Garapin F, Fleckenstein B, Bodemer W.** 1985. Terminal repetitive sequences in herpesvirus saimiri virion DNA. J. Virol. **55**:133–139.
11. **Chang Y, Cesarman E, Pessin MS, Lee F, Culpepper J, Knowles DM, Moore PS.** 1994. Identification of herpesvirus-like DNA sequences in AIDS-associated Kaposi's sarcoma. Science **266**:1865–1869.
12. **Moore PS, Gao SJ, Dominguez G, Cesarman E, Lungu O, Knowles DM, Garber R, Pellett PE, McGeoch DJ, Chang Y.** 1996. Primary characterization of a herpesvirus agent associated with Kaposi's sarcomae. J. Virol. **70**:549–558.
13. **Russo JJ, Bohenzky RA, Chien MC, Chen J, Yan M, Maddalena D, Parry JP, Peruzzi D, Edelman IS, Chang Y, Moore PS.** 1996. Nucleotide sequence of the Kaposi sarcoma-associated herpesvirus (HHV8). Proc. Natl. Acad. Sci. U. S. A. **93**:14862–14867.
14. **Alexander L, Denekamp L, Knapp A, Auerbach MR, Damania B, Desrosiers RC.** 2000. The primary sequence of rhesus monkey rhadinovirus isolate 26-95: sequence similarities to Kaposi's sarcoma-associated herpesvirus and rhesus monkey rhadinovirus isolate 17577. J. Virol. **74**:3388–3398.
15. **Virgin HWt, Latreille P, Wamsley P, Hallsworth K, Weck KE, Dal Canto AJ, Speck SH.** 1997. Complete sequence and genomic analysis of murine gammaherpesvirus 68. J. Virol. **71**:5894–5904.
16. **Orzechowska BU, Powers MF, Sprague J, Li H, Yen B, Searles RP, Axthelm MK, Wong SW.** 2008. Rhesus macaque rhadinovirus-associated non-Hodgkin lymphoma: animal model for KSHV-associated malignancies. Blood **112**:4227–4234.
17. **Wong SW, Bergquam EP, Swanson RM, Lee FW, Shiigi SM, Avery NA, Fanton JW, Axthelm MK.** 1999. Induction of B cell hyperplasia in simian immunodeficiency virus-infected rhesus macaques with the simian homologue of Kaposi's sarcoma-associated herpesvirus. J. Exp. Med. **190**:827–840.
18. **Ascherio A, Munger KL.** 2010. Epstein-Barr virus infection and multiple sclerosis: a review. J. Neuroimmune Pharmacol. **5**:271–277.
19. **Spooren A, Kolmus K, Laureys G, Clinckers R, De Keyser J, Haegeman G, Gerlo S.** 2011. Interleukin-6, a mental cytokine. Brain Res. Rev. **67**:157–183.
20. **Hendriks JJ, Teunissen CE, de Vries HE, Dijkstra CD.** 2005. Macrophages and neurodegeneration. Brain Res. Rev. **48**:185–195.
21. **Koning N, Bo L, Hoek RM, Huitinga I.** 2007. Downregulation of macrophage inhibitory molecules in multiple sclerosis lesions. Ann. Neurol. **62**:504–514.